THREE-DIMENSIONAL VISUALIZATION OF COATED VESICLE FORMATION IN FIBROBLASTS

JOHN HEUSER, with the technical assistance of LOUISE EVANS

From the Department of Physiology, School of Medicine, University of California, San Francisco, California 94143

ABSTRACT

Fibroblasts apparently ingest low density lipoproteins (LDL) by a selective mechanism of receptor-mediated endocytosis involving the formation of coated vesicles from the plasma membrane. However, it is not known exactly how coated vesicles collect LDL receptors and pinch off from the plasma membrane. In this report, the quick-freeze, deep-etch, rotary-replication method has been applied to fibroblasts; it displays with unusual clarity the coats that appear under the plasma membrane at the start of receptor-mediated endocytosis. These coats appear to be polygonal networks of 7-nm strands or struts arranged into 30-nm polygons, most of which are hexagons but some of which are 5- and 7-sided rings. The proportion of pentagons in each network increases as the coated area of the plasma membrane puckers up from its planar configuration (where the network is mostly hexagons) to its most sharply curved condition as a pinched-off coated vesicle. Coats around the smallest vesicles (which are icosahedrons of hexagons and pentagons) appear only slightly different from "empty coats" purified from homogenized brain, which are less symmetrical baskets containing more pentagons than hexagons. A search for structural intermediates in this coat transformation allows a test of T. Kanaseki and K. Kadota's (1969. *J. Cell Biol.* **42**:202–220.) original idea that an internal rearrangement in this basketwork from hexagons to pentagons could "power" coated vesicle formation. The most noteworthy variations in the typical hexagonal honeycomb are focal juxtapositions of 5- and 7-sided polygons at points of partial contraction and curvature in the basketwork. These appear to precede complete contraction into individual pentagons completely surrounded by hexagons, which is the pattern that characterizes the final spherical baskets around coated vesicles.

KEY WORDS coated vesicles · adsorptive endocytosis · surface replicas · freeze-dried fibroblasts

Adsorptive endocytosis of proteins and hormones appears in most cells to operate by the formation of coated vesicles from the plasma membrane. During this process, membrane-bound receptors for these proteins become associated with coated pits in the plasma membrane, after which these coated pits pinch off from the membrane to become coated vesicles, which in turn transport the protein to the lysosomal system or elsewhere inside the cell (for a recent review, see reference 16; for specifics, see references 1–4, 7, 10, 13–16, 31–34, 39, 47–49, 52, and 55).

J. CELL BIOLOGY © The Rockefeller University Press · 0021-9525/80/03/0560/24 $1.00
Volume 84 March 1980 560–583

However, it is not known how coated pits form or how their coats change as they pinch off from the plasma membrane to become coated vesicles. The views of coated pits shown in this report display the organization of the coat more clearly than heretofore possible and illustrate the variety of geometrical forms that it can assume. These data set constraints on the models that can be proposed for coated vesicle formation.

In addition, the technique of specimen preparation used here produces images that look like a cross between thin-section images and freeze-fracture images, so it becomes possible to look for structures that might link the coat to membrane receptors and to cytoplasmic filaments.

MATERIALS AND METHODS

Cell Culture

Fibroblasts originally isolated by trypsinization from Balb C mouse embryos were used within four passages and plated into 60-mm tissue culture dishes (Falcon Labware, Div. of Becton, Dickinson & Co., Oxnard, Calif.) containing a number of 4-mm^2 fragments of No. 1 coverglass. They were maintained in Dulbecco's modified Eagle's essential medium with 10% fetal calf serum and allowed to settle down and spread on the glass cover slips for 18 h before each experiment.

Freezing and Replication

Cultures were quick-frozen by mounting individual coverslips on aluminum disks that are attached to the end of a plunger device originally designed to catch exocytosis in isolated frog muscles. This plunger rapidly drops causing the samples to strike a pure copper block that is cooled to the temperature of liquid helium (see reference 27 for details of the construction and operation of this device). In our experiments, this method produced frozen tissue-culture cells embedded in microcrystalline ice in which the crystals were <20 nm as a result of the extremely rapid freezing. To avoid crushing the cells and shattering the coverglasses when the plunger made contact with the copper block, we mounted the coverglasses on a soft, spongy matrix composed of slices of aldehyde-fixed rat lung. (The lung was fixed in 2% glutaraldehyde in water, sliced to a thickness of 0.8 mm with a Smith-Farquhar tissue chopper, and stored in distilled water, often for weeks, before use.) The slices of lung became bonded to the surface of the aluminum disks as they froze and thus served as supports and carriers for the frozen coverglasses. The disks could then be mounted on the standard rotary specimen stage in a freeze-fracture device (Balzers Corp., Nashua, N. H.).

Once a vacuum of 10^{-6} torr or greater was achieved in this device, the specimens were warmed to −100°C and fractured in the standard way. Then the tissue was etched for 2.5 min, which removed 0.1–0.25 μm of water from the fractured surface. After etching, the samples were rotary replicated by evaporating carbon-platinum onto them from a standard electron-beam gun mounted at 24° to the specimen plane while the specimen was rotating at 60 rpm. The resulting platinum replica was stabilized by 5 s of rotary deposition of pure carbon from a gun mounted at 75° to the specimen plane. The coverglass was then removed from the vacuum and floated off the lung onto 30% hydrofluoric acid in water, which promptly released the replica from the glass surface. The replica was then floated sequentially through distilled water, full-strength household bleach, and two more water washes before being picked up on 75-mesh Formvar carbon-coated grids.

Microscopy

The replicas were examined in a JEOL 100B or 100C electron microscope operating at 100 kV. The high accelerating voltage was used to reduce heating of the replica, to minimize recrystallization, and to reduce contrast in the final photographic negatives. Stereo pairs were obtained with a high-resolution, top-entry goniometer stage tilted through ± 7° for all magnifications. Micrographs were examined in negative contrast, i.e., by projecting the original electron microscope negatives or by photographically reversing them before printing to make the platinum deposits appear white and the background dark. This reverse contrast enhanced the three-dimensional appearance of the images, as if the cells were illuminated by a gentle, diffuse "moonlight." The samples appeared much as they do in the standard secondary mode of scanning electron microscopy.

RESULTS

While attempting to visualize attachment points of actin filaments to the inside of the plasma membrane in fibroblasts prepared as described above, we quite fortuitously obtained a number of glimpses of polygonal networks that appeared to lie under the filaments immediately against the inside of the plasma membrane (Fig. 1). These seemed likely to be unusual views of the "basketwork" that Kanaseki and Kadota (29) first saw around coated vesicles, though now on the inside of the plasma membrane. Roth and Porter (49), in their original description of protein endocytosis by coated vesicles, showed that coated areas of the plasma membrane exist and predicted that these would be precursors of coated vesicles. Kanaseki and Kadota (29) predicted further that the coat under the plasma membrane would be formed of pure hexagons when it was flat, and that it would "power" the membrane invagination by rearranging some of its hexagons into pentagons, thus forming the geodesic basket they observed around pinched-off coated vesicles. The views of basketworks shown in Fig. 1 were obtained from cells that had been distended in their last minute before freezing by a rinse in distilled water. This was done to dilute soluble cytoplasmic components and open up the view obtained by deep etching. Cells that were quick frozen and etched without this preliminary hypotonic shock displayed such a high concentration of unetchable granular material in their cytoplasm that views such as Fig. 1 were quite impossible to obtain (cf. reference 40).

A second way to clear the cytoplasm for deep

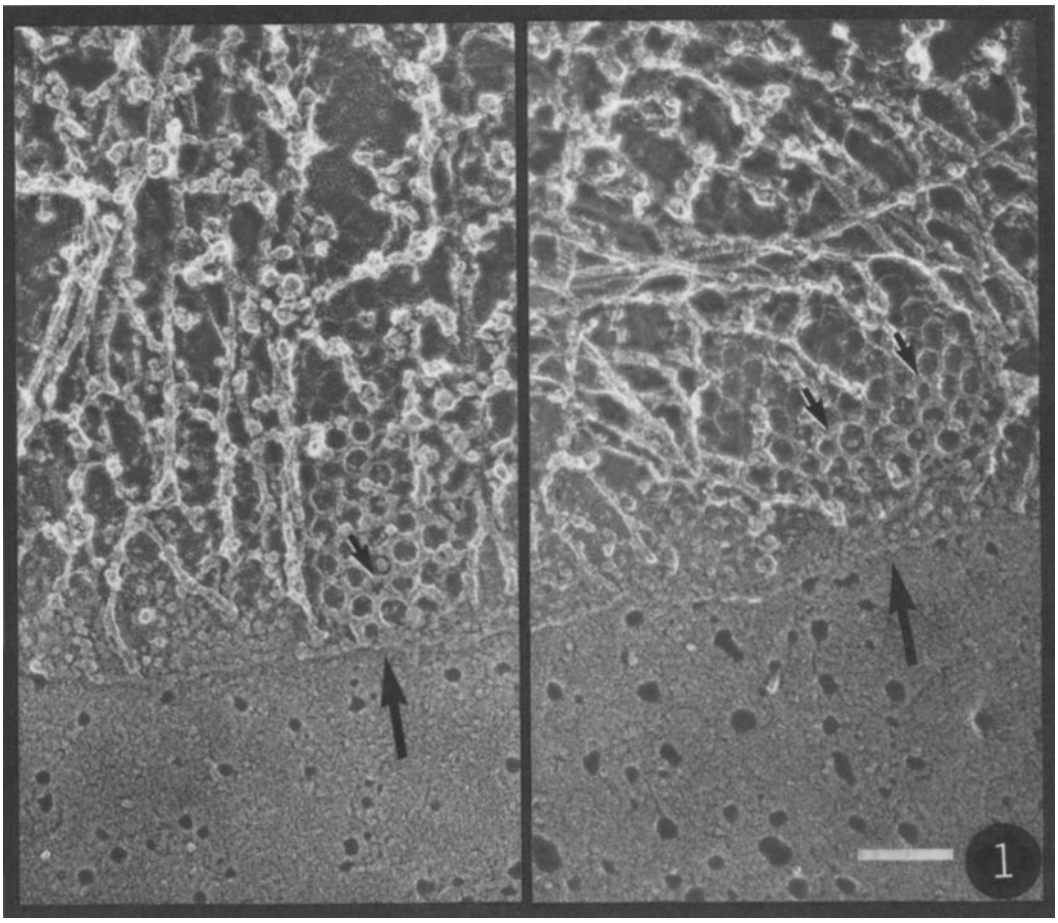

FIGURE 1 Freeze-etch view of the inner surface of the fibroblast plasma membrane from a cell that had been quick-frozen without fixation and then freeze-fractured before etching. Actin filaments can be seen amid unidentified granular material in the cytoplasm above. The E-fracture face of the plasma membrane can be seen below, badly pitted by the long etching. Near the "shoreline" where the inner membrane surface begins (large arrows) are two polygonal "honeycombs" visible under the filaments. The honeycombs are composed largely of hexagons, with a few juxtapositions of five- and seven-member rings (small arrows). Bar, 0.1 μm. × 126,000.

etching was to fix the cells with 1% glutaraldehyde in phosphate-buffered saline and then wash them in distilled water. This totally eliminated salts that may have formed part of the unetchable granular material, but the aldehyde fixation had certain pitfalls that will be illustrated more fully in a later report (J. Heuser and M. W. Kirschner, manuscript submitted). Soluble components of the cytoplasm appeared to become cross-linked to insoluble components because something obscured, or at least decorated, the cytoplasmic filaments and membrane surfaces. In spite of this, aldehyde-fixed cells yielded the most complete views of basketworks against the inside of the plasma membrane, possibly because fixed cells fractured more favorably with the technique we used. Often, it appeared that almost everything in the culture had been removed, leaving only the parts of the fibroblast plasma membranes that had been in direct contact with the coverglass. This afforded views, such as seen in Fig. 2, of the true cytoplasmic surface of the plasma membrane. On that surface could be found many basketworks in a variety of curvatures. Immunocytochemistry has shown that coated pits are as abundant on the bottom of the cell as on the top, which is exposed to the most

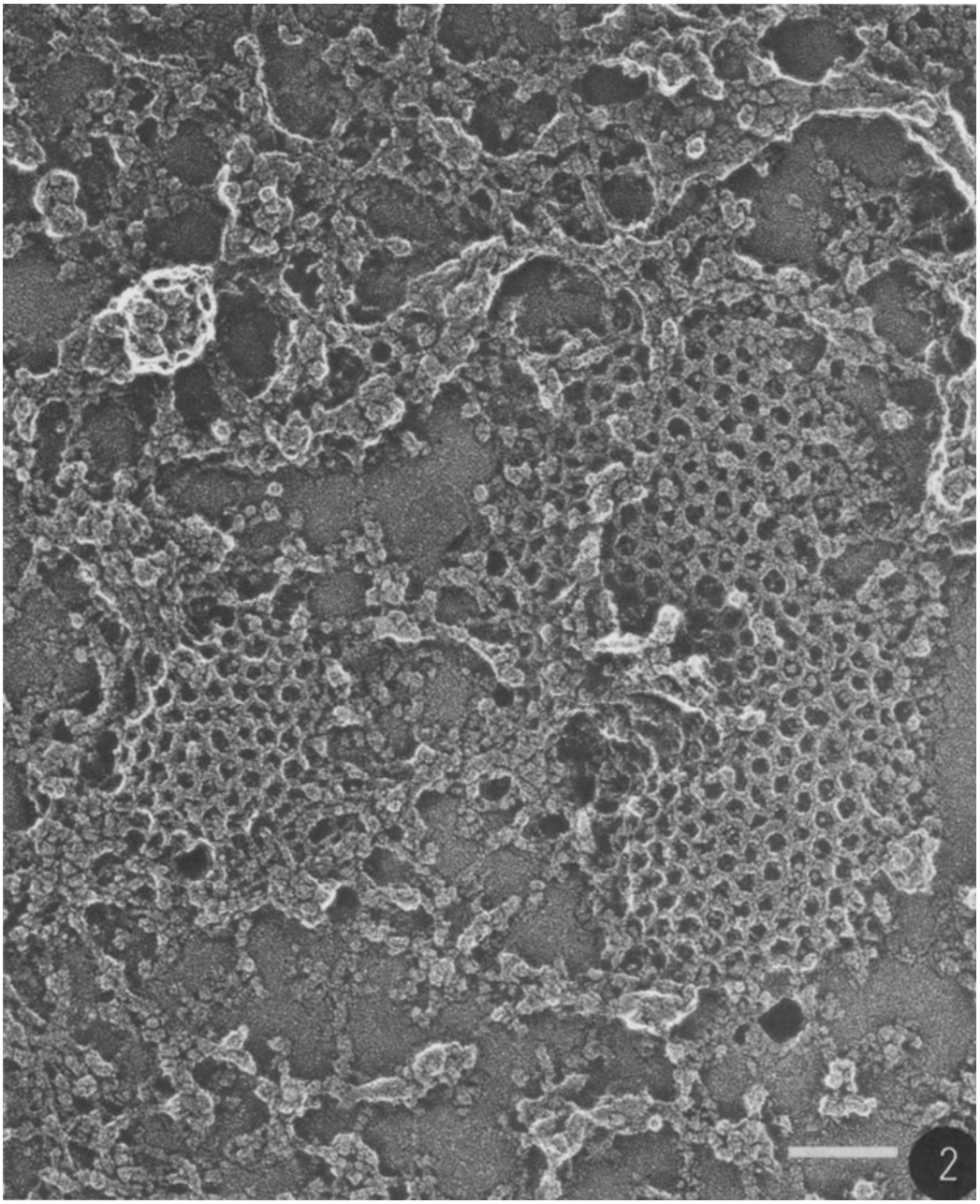

FIGURE 2 View of the inside of the plasma membrane from a fibroblast fixed with aldehydes before preparation as in Fig. 1. Submembranous filaments are coarsened and obscured by a coagulum, but, for unknown reasons, the honeycombs stand out even more clearly. Again, a few five- and seven-sided polygons are found side by side among the hexagonal majority. Bar, 0.1 μm. × 140,000.

tissue culture fluid (4).

The rotary replicas of this membrane surface showed the overall organization of the basketworks quite clearly (Fig. 3). They appeared to be composed of honeycombs with ~8.5-nm walls or struts linked predominantly into hexagons, with a few pentagons and heptagons interspersed, as will be illustrated later. These polygons were so small

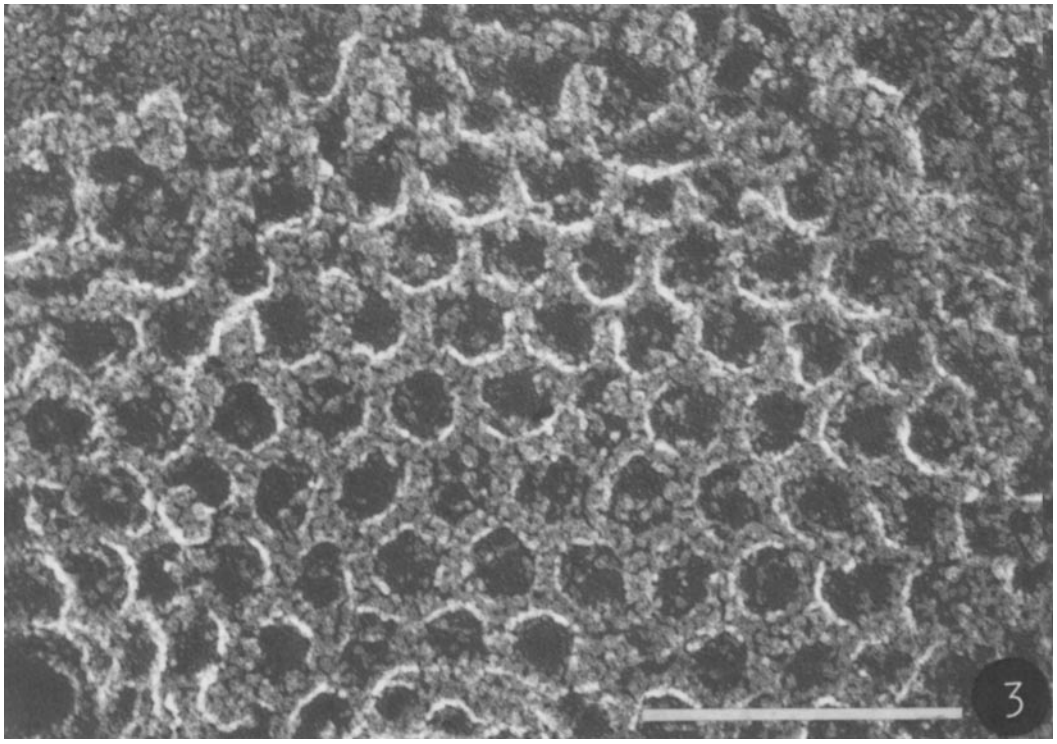

FIGURE 3 High magnification of the honeycomb network shows that it is composed of raised material, uniformly 7 nm wide, and linked into tight polygons, each 30-nm in diameter. The granular background of the platinum replica is here about 2 nm. Bar, 0.1 μm. × 420,000.

(~30 nm) and the shadowing angle so flat, that it was difficult, in these replicas, to see through the baskets to the plasma membrane underneath. The surface detail of the basket itself, however, was quite clear, and there were no overlapping images of front and back sides such as those that complicate three-dimensional electron microscopy of stained tissues, which often need optical diffraction to be deciphered.

The submembranous basketworks ranged from <10 nm to >300 nm in diameter. Consequently, they were composed of a variable number of polygons or facets (from as few as 8 to more than 200 in the largest basketworks) as is shown in Fig. 4. The arrow in this figure points to the mean number of facets, which was 61, with a broad standard deviation of ± 40. This mean is equivalent to an average diameter of 220 nm, which is comparable to the size of coated pits visualized in fibroblasts by other techniques (1, 2, 4). The observation of a continuous range of sizes suggested that the submembranous basketworks start as just

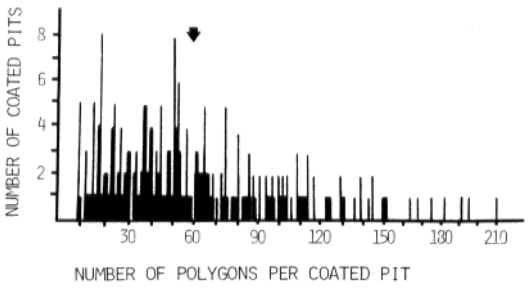

FIGURE 4 Histogram illustrating how often coated pits of various sizes were found. Size is expressed as the number of polygons per coated pit. 256 examples from several dozen fibroblasts are displayed. The mean number of polygons is 61 (arrow), which is equivalent to a basketwork 220 nm in diameter. However, the distribution was slightly skewed, as a result of a few very large basketworks that may have been confluent pairs. Therefore, the median of 52 polygons may be a better index of the average size of these coated pits, which would be 190 nm. (Note that a basketwork 200 nm in diameter would ball up into a coated vesicle 100 nm in diameter, which would be typical of those found in fibroblasts.)

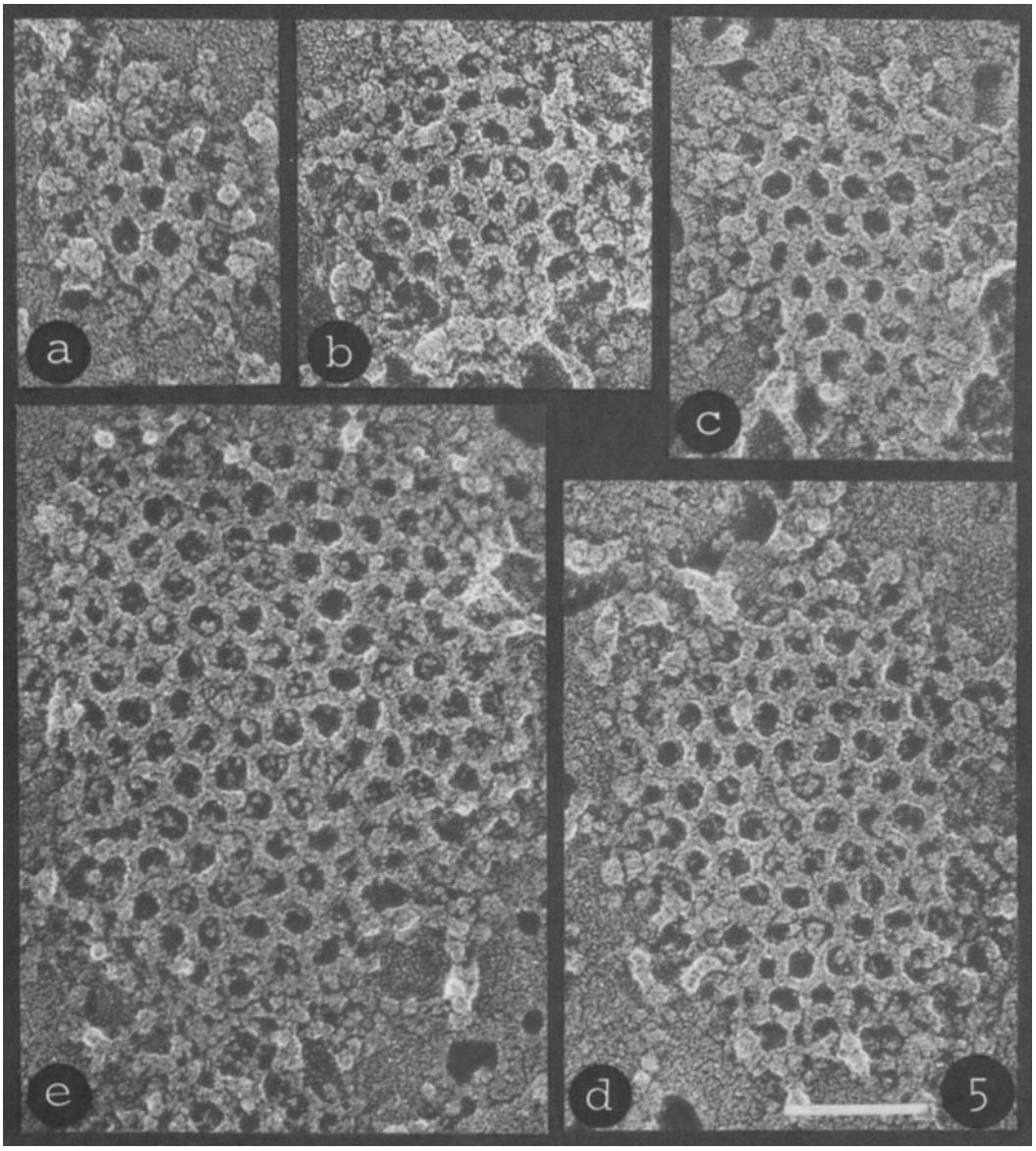

FIGURE 5 Selected examples from the various sizes of basketwork found, arranged to suggest continuous, progressive growth (from *a* to *e*). The peripheral margins of the basketworks are invariably composed of incomplete polygons, regardless of how large the overall basketwork is. Bar, 0.1 μm. × 200,000.

a few polygons and grow by the progressive addition of more. Closer examination gave no indication that growth was by coalescence of several small patches of polygons; that is, small patches were never found near one another, nor was there any indication that basketworks grew in "quantal jumps" of dozens of polygons at a time, as might be expected if whole coated vesicles (or whole "empty baskets," which will be described later) could join the basketworks one at a time. Instead, the histogram of sizes (Fig. 4) was smooth enough to suggest that growth was progressive and continuous.

Fig. 5 displays five basketworks that were typical of the various sizes observed. Searching the margins of these basketworks for an indication of

how they might grow revealed that their periphery was usually ragged and composed of incomplete polygons bordered by amorphous material, which suggested that growth is most probably by the piecemeal assembly of polygons around the periphery.

The basketworks displayed in Fig. 5 were among the flattest that could be found. It was more common to find them in various degrees of curvature. The examples displayed in Fig. 6 include the whole range of images that would be expected for a sequence of endocytosis. (Of course, there was no way to assign a time arrow to this sequence; it could represent the reverse process, i.e., coated vesicle exocytosis, if such a process occurs in fibroblasts.) The various degrees of curvature could be evaluated much more accurately by tilting the replica ± 7° in the electron microscope and making stereo pairs of individual basketworks such as are displayed in Fig. 7. These dramatically illustrate that even the flattest baskets had a small degree of inward curvature, and many were complete hemispheres.

These rotary-replicated images were so clear that they allowed a direct test of Kanaseki and Kadota's (29) idea that an internal rearrangement of the coat from hexagons to pentagons is associated with membrane curvature. To evaluate this possibility, 256 particularly clear examples of coated pits were arranged into three categories according to their degree of curvature: flat, slightly curved, and very curved. The categories included examples such as those in Figs. 5, 6*a*, and 7*a* (flat); Figs. 6*b* and 7*b* (slightly curved); and Figs. 6*c* and 7*c* (very curved). Then, the numbers of hexagons and pentagons were counted in each of these examples. Finally, the mean proportion of pentagons (± 1 SE) was plotted for each of the categories (Fig. 8). This illustrates that flat coats had a preponderance of hexagons, whereas more curved coats had a significantly higher proportion of pentagons.

We may presume, from basic crystallographic considerations, that a completely enclosed, spherical network of polygons will include at least 12 pentagons. Because there were 61 ± 40 polygons in the basketworks studied, the proportion of pentagons should be hypothetically have approached 12/60, or 20%, as they curved more and more. Thus, it was odd to find that the very curved ones, which often appeared as near hemispheres in stereo, had only ~3% pentagons. This value may have been low because of counting errors inasmuch as it was difficult to recognize pentagons along the steep slopes of the more curved networks. But this value may have been this low because there is actually more flexibility in the coat than in a rigid, spherical crystal, and fewer pentagons would be necessary to form a closed surface. Other evidence for such flexibility was indeed present. Some basketworks that were composed entirely of hexagonal facets appeared unmistakably curved when viewed in stereo.

Nevertheless, in the most extremely curved baskets, a very high proportion of pentagons was observed (>50%). Fig. 9 illustrates such baskets obtained from homogenates of bovine brain by standard methods (30, 44) that were less than 1/10 the diameter of coated vesicles in fibroblasts and, thus, much more acutely curved. Correspondingly, they were composed of a much smaller number of facets. Stereo electron microscopy of these empty baskets (Fig. 10) provided three-dimensional views that fully substantiated the predictions about their structure made by Crowther et al. (9) from negatively stained images, but unlike the negatively stained images, the freeze-etched replicas introduced none of the ambiguity that results from superimposition of the image of the back side of the basket.

Intermediates in Basket Curvature

Because the shape of each individual polygon was easily discernible in these various views of coated pits, it could be expected that this technique would reveal exactly what happens when a facet in the basketwork rearranges from a hexagon to a pentagon. Unfortunately, thus far, no definitive coat transformation intermediate has been identified. The only possible clue was that many of the larger, flatter sheets, such as the one in Fig. 11, displayed pentagons near heptagons, which, as a result of their increased number of sides, were obviously larger than the surrounding hexagons

FIGURE 6 Selected examples from the various degrees of curvature found, arranged as a progressive increase in curvature from *a* to *e*, to suggest the sequence of invagination that would be expected for coat-mediated endocytosis. Almost fully formed coated vesicles are shown in *f* to *h*. Bar, 0.1 μm. × 200,000.

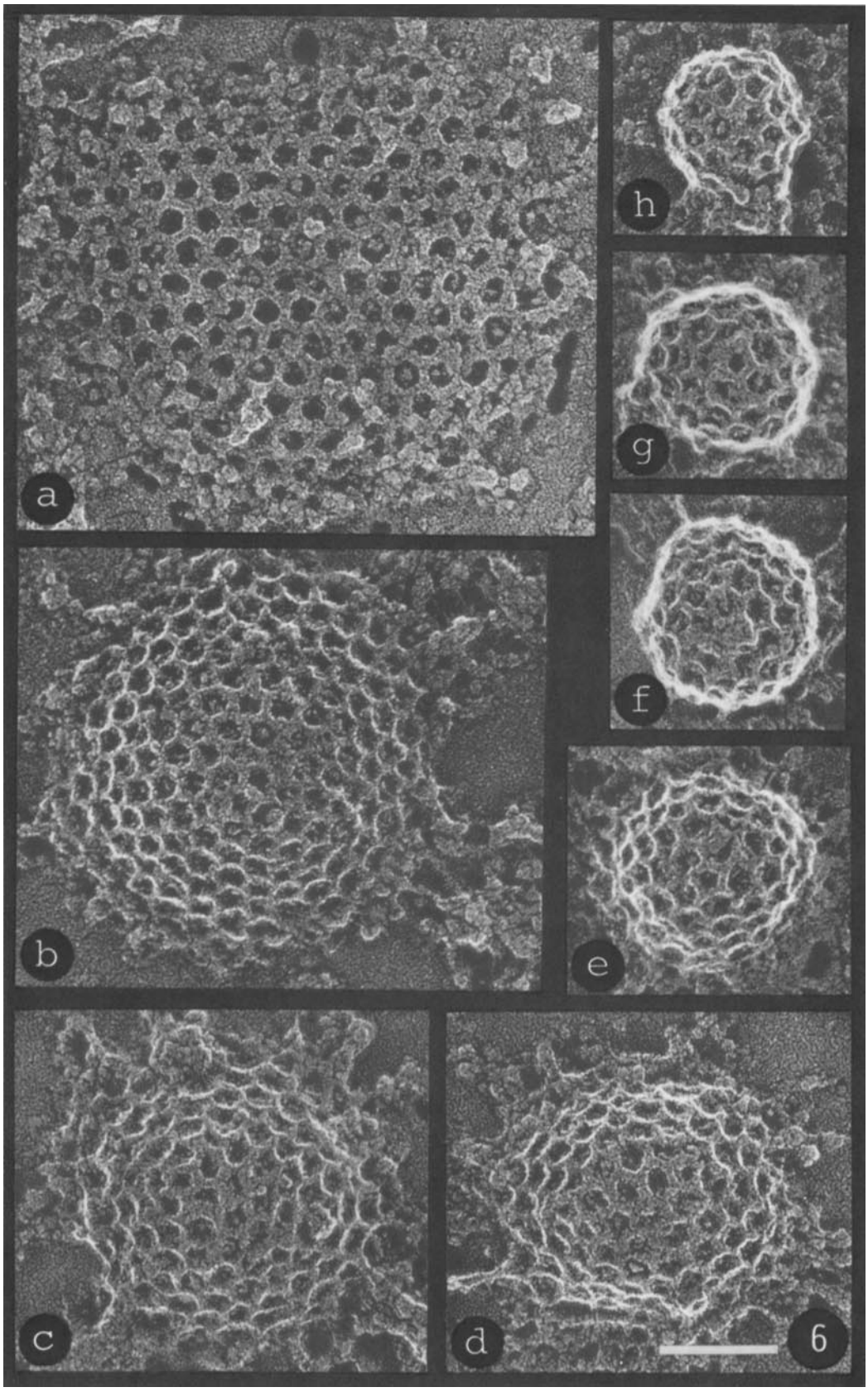
a
b
c
d
e
f
g
h
6

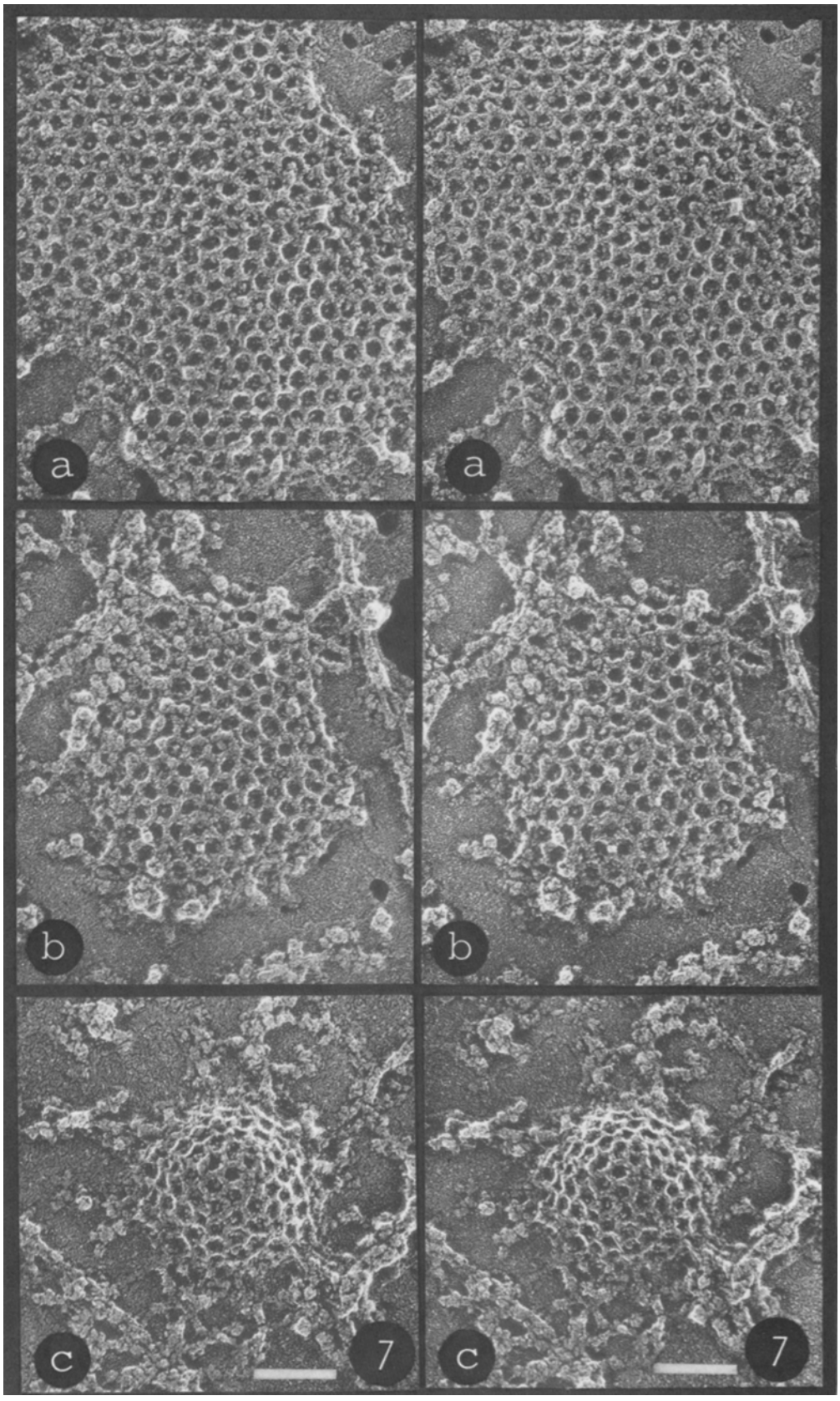
a
a
b
b
c
7
c
7

and thus compensated for the reduced size of the neighboring pentagons.

Closer inspection of the lattices in which these "five-seven dislocations" could be found (Fig. 12) revealed that they invariably occurred where one row of hexagons stopped and the two rows that had flanked it came together. The pentagon was the last facet of the terminating row, and the adjacent heptagon was a member of one or the other flanking row. Such a transition from three to two rows meant that the basketwork became narrower on one side than the other. A search through an old biology library showed that identical five-seven dislocations occur in beehives and in diatoms that grow asymmetrically. Invariably, where a new row of hexagonal cells is added in the midst of two others, it begins with a pentagon flanked by a heptagon.

As yet, it is not clear what relation these five-seven lattice dislocations have to coat curvature, if any. When they occur in beehives, the honeycombs do not curve. However, when models were built from hexagonal chicken wire, removing a row of hexagons produced a five-seven pair that

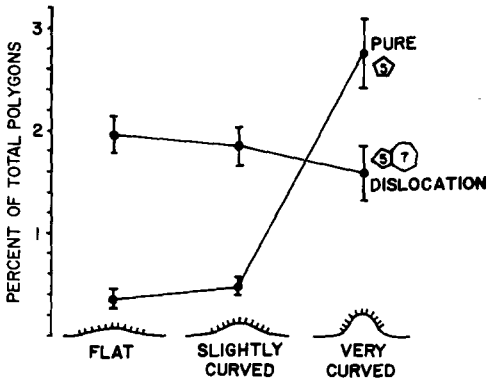

FIGURE 8 Relative abundance of pentagons and "five-seven dislocations" in coated pits of various degrees of curvature. Pentagons become significantly more abundant as the basketworks curve, confirming Kanaseki and Kadota's (29) original idea (error bars indicate ± 1 SE). Five-seven dislocations, however, are relatively abundant at all degrees of curvature. Not apparent in the statistics is the evidence that these forms are intermediates in coat rearrangement, which is described in Results in relation to Figs. 10–13.

was strained, and the strain led to a slight degree of curvature as is illustrated stereoscopically in Fig. 13. These models also showed that the spatial discontinuity introduced by terminating a row of facets with a pentagon could not be alleviated merely by forming one adjacent heptagon; all the hexagons around it also were severely strained. For this reason, we included the example of an *in situ* five-seven lattice discontinuity shown in Fig. 12 (*top*), in which the hexagon next in line to the heptagon appears stretched and distorted. This could be a natural manifestation of a strain that would lead to a curvature such as that seen in Fig. 13.

The *in situ* examples in Fig. 12 also include an instance of two five-seven discontinuities occurring adjacent to each other, not an uncommon finding. It represents a point at which two rows stopped, and the lattice was consequently even more contracted and curved. Further experimenting with chicken wire also illustrated that terminating one more row, so that a total of three rows were stopped in a staggered sequence (which was equivalent to removing the pie-shaped piece illustrated in Fig. 13), resulted in even greater curvature of the chicken wire and the formation of a totally new lattice in which heptagons were gone and nonadjacent rows ran completely together at 60° to each other such that only one pentagon was left in their midst. Fig. 12 (*bottom*) is an example of such an interruption of three rows at a lone pentagon found *in situ* in a moderately curved basketwork.

Model building raised the possibility that coat curvature in vivo might involve just such a progressive elimination of rows, and that five-seven dislocations might be significant intermediates in this process. In the search for evidence in support of this possibility, the relative abundance of five-seven dislocations in coats of different curvature was determined in the same three groups of coats used to make Fig. 8. The results illustrate that coincident with the increase in abundance of pentagons that accompanied increased curvature was a slight decrease in the abundance of five-seven dislocations. They represented 3% of all the facets in flat and moderately curved baskets, but were

FIGURE 7 Three stereo pairs of basketworks with different degrees of curvature, from *a*, the flattest (which are not completely flat when seen in stereo), to *c*, the stage approaching a hemisphere, aptly called a campanulate invagination of the plasma membrane. Bars, 0.1 μm. × 130,000.

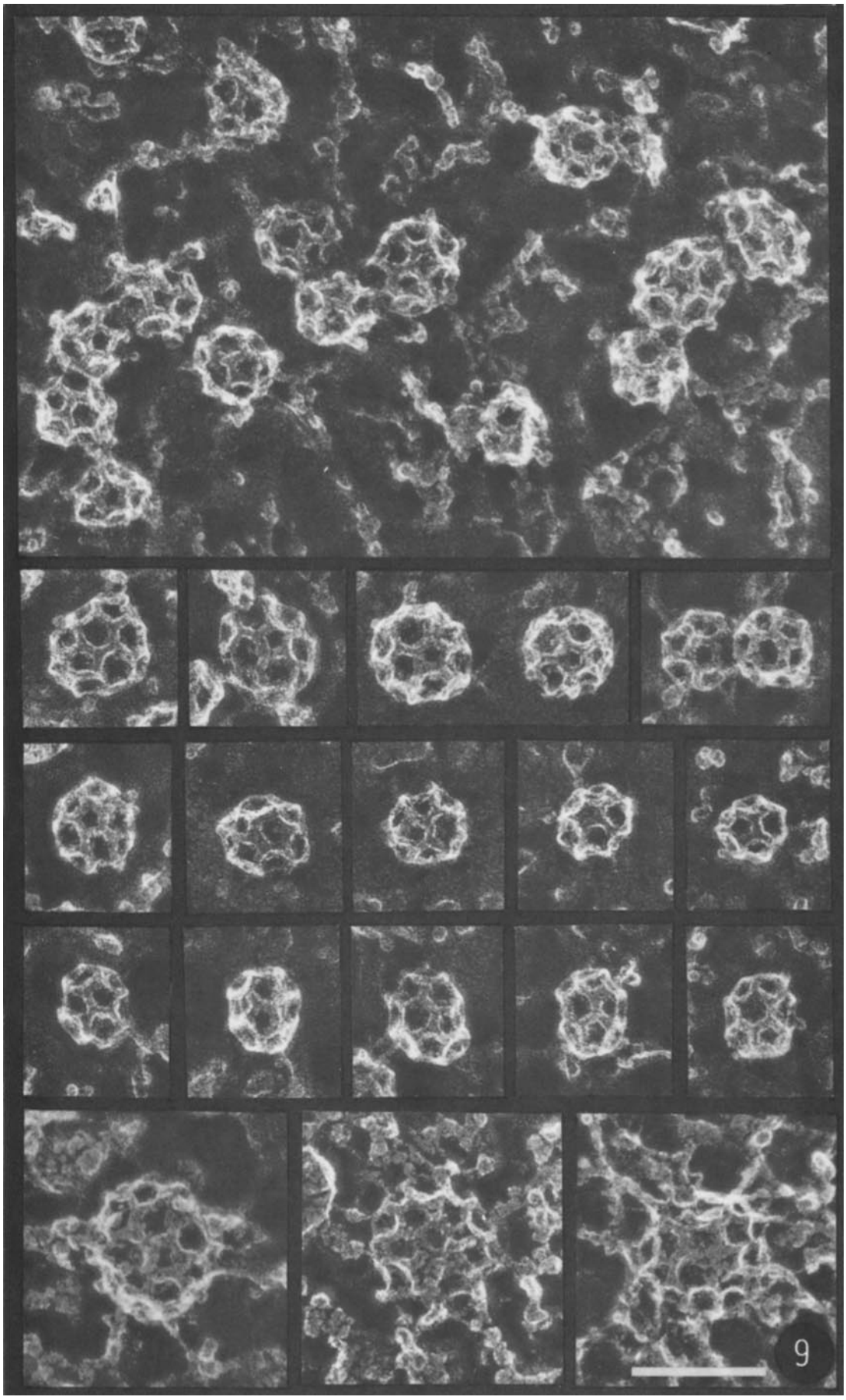
9

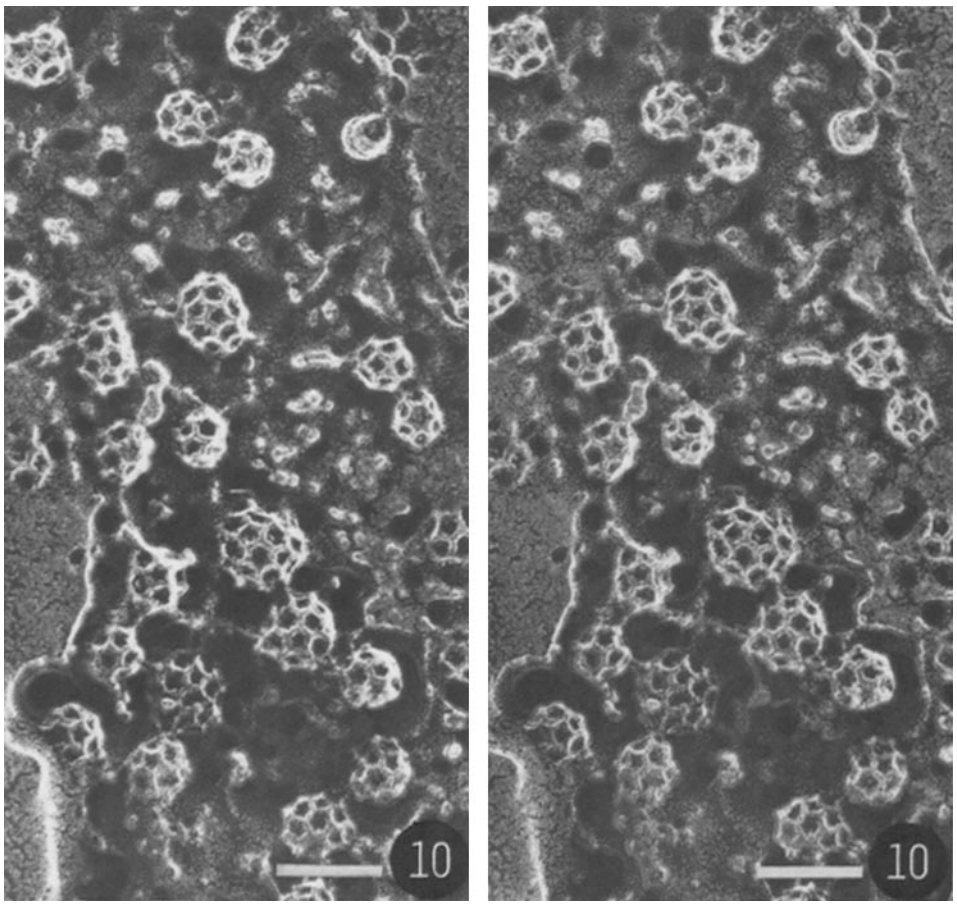

FIGURE 10 Stereo pair of the empty baskets isolated from brain and etched just enough to expose half of the basket and to obtain a clear, unequivocal view of their polygonal composition. Bars, 0.1 μm. × 139,000.

entirely absent from a large fraction of the very curved group. Furthermore, it was obvious from simple inspection of preparations such as those in Figs. 9 and 10 that seven-sided rings were relatively rare in small spherical baskets.

Such hints of a decline in the relative abundance of five-seven dislocations during curvature raised the possibility that in life such distortions might "mend" into more curved, pure, five-sided insertions; but we have no explanation of how such mending could occur in the midst of an otherwise hexagonal lattice.

It is perhaps worth adding, in this regard, that pentagons were particularly common around the

FIGURE 9 The appearance of "empty baskets" isolated from brain and prepared by the freeze-etch and replication method used for fibroblasts. The baskets are seen to be composed of polygons with facets and struts of the same size found on the inside of fibroblast coated pits. As a result of their extremely sharp curvature, however, these small, isolated baskets display a much higher proportion of pentagons than the large coated pits. At the bottom, at the same magnification, are three examples of the smallest baskets that were found *in situ*, amid the unidentified granular material that abounds inside quick-frozen fibroblasts. These *in situ* baskets appear to be too small to accommodate a membranous vesicle, and thus may also be empty baskets. Bar, 0.1 μm. × 230,000.

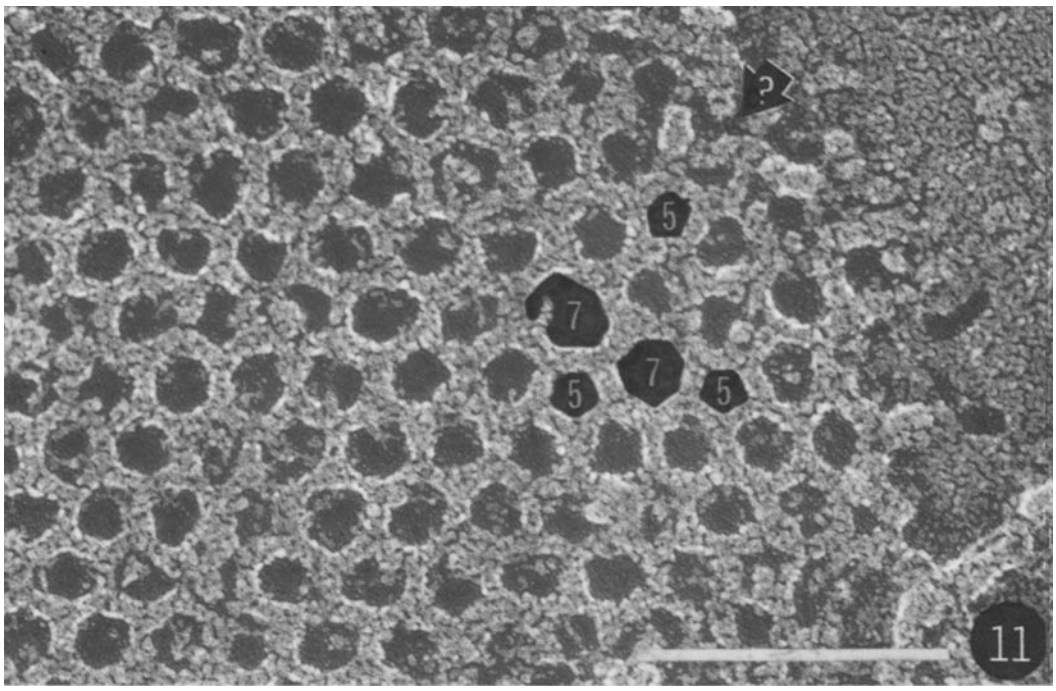

FIGURE 11 Higher magnification of the edge of one large coated pit showing two examples of the juxtapositions of five- and seven-member rings that invariably occur at lattice discontinuities in the otherwise hexagonal basketworks. Also shown is one five-sided ring near the periphery, where adjacent polygons are incomplete and distorted but in many instances appear to be portions of heptagons. Bar, 0.1 μm. × 360,000.

edges of the basketworks, where adjacent polygons were still incomplete. In these cases, it was impossible to tell whether they were destined to be pure pentagons or whether a seven-sided ring might have been in the process of forming adjacent to them. Thus, we could not assign them to either group nor include them in the calculations of the relative abundance of the pure pentagon's and the five-seven dislocations in Fig. 8. It may, however, be significant that such edge pentagons constituted a considerable portion of the dislocations that occurred: 46% in flat, 48% in moderately curved, and 36% in very curved dislocations. Subjectively, many of these pentagons appeared as though they were going to become five-seven pairs, so that it seemed that lattice dislocations and mending occurred more frequently around the growing edges of the baskets. On the other hand, if even a few of these edge pentagons were destined to become completely surrounded by hexagons, it would be necessary to conclude that some degree of curvature can be built into the coats as soon as they form. Such a "prefabrication" of the curvature might not always be the case, however. Often, very flat basketworks occurred that were quite large and almost entirely hexagonal. Unless these prove to be some sort of dead end, they would have to rearrange themselves into pentagons if they were ever to curve into coated vesicles.

Outside Views of Coated Pits

What must have been the outside of coated pits in the plasma membrane could be seen by simply freeze-drying the fibroblasts without fracturing them open. This revealed broad expanses of the upper surfaces of these cells (Fig. 14). Rotary platinum replicas viewed in transmission electron microscopy provided images of these surfaces that were considerably higher in resolution than comparable scanning electron microscopic images of gold-coated cells, revealing that the surfaces of the fibroblasts were covered with a variety of small bumps that were about the size of intramembrane particles, apparently scattered at random. Previously, we have shown that this procedure can display membrane receptors for neurotransmitters of similar size on the surface of certain postsynaptic membranes and can show when such recep-

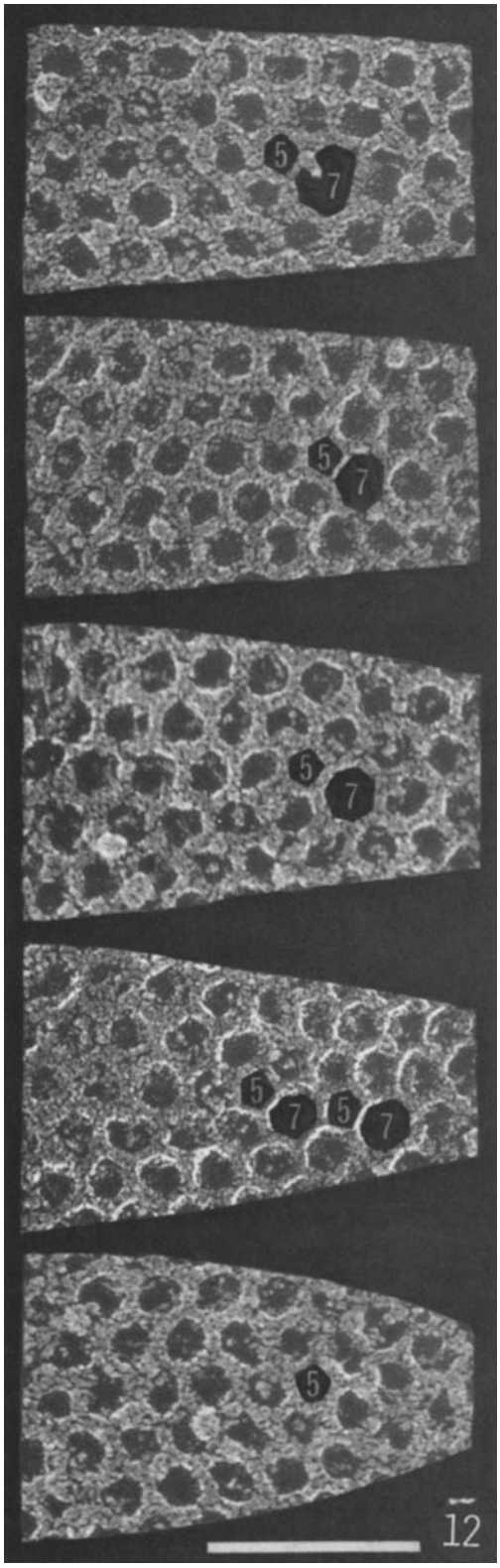

tors assume a nonrandom distribution (28).

The surfaces of fibroblasts also displayed other, much larger globules (~250 Å in diameter), which were extremely smooth and spherical (Fig. 15), which looked exactly like recently published images of freeze-dried, low density lipoprotein (LDL) molecules (22). The ones seen in fibroblasts appeared to be linked to receptors, because they typically occurred in distinct clusters of various sizes and degrees of compaction. Stereomicroscopy revealed that the tightest clusters were deeply invaginated (Fig. 15). (Similar 250-Å droplets were found here and there on the bare surface of the coverglass, but their concentration at indentations on the fibroblast surface did not seem to be an artifact of aldehyde fixation because fibroblasts quick-frozen without fixation also displayed similar clusters of globules in shallow depressions of the plasma membrane (Fig. 14 *e*), albeit less clearly because of a residue of tissue culture medium left after freeze-drying.) The indentation of the LDL clusters suggests that their receptors were already linked to coated pits because all indentations of this size were coated when seen from the inside. This would fully agree with the results of earlier immunocytochemistry of ferritin-labeled LDL viewed in thin sections (1) and with subsequent visualization of deep-etched fibroblasts prepared by a freezing method slower and more deleterious than that used by us (41). One advantage of our method was that the LDL molecules per coated pit could be counted directly; the number ranged from 20 to 40 in the cells we viewed.

It was also possible to obtain outer views of the basketworks by treating fibroblasts with Triton X-100 before freeze-drying them. 1–3 h in 1% Triton X-100 at 37°C was necessary to rid the fibroblasts of all traces of their membrane after they were fixed, but this did not appear to alter their cytoarchitecture. Left were stress fibers, cortical microfilaments, and, of particular interest in this context, 0.1–0.3-μm cuplike depressions composed of a

FIGURE 12 Cropped portions of five basketworks, chosen to illustrate how a five-seven juxtaposition marks a spot of lattice contraction. At this spot, one row of polygons narrows and terminates with a pentagon, and one of the two rows adjacent to it contains a heptagon to fill in the space where the two rows come together. Two rows are eliminated by two successive five-seven juxtapositions. When three rows are eliminated, one pentagon is seen at the end of the central row, with the two adjacent rows coming together at a distorted hexagon. The rows may be seen more easily by raising the edge of the page. Bar, 0.1 μm. × 310,000.

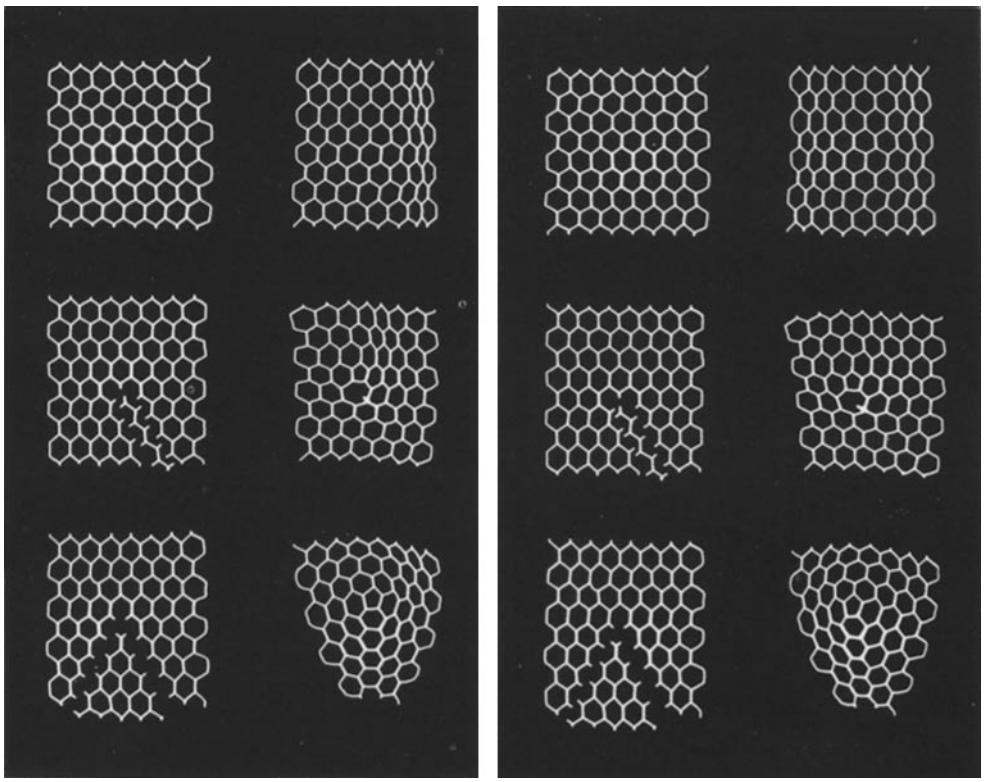

FIGURE 13 Stereo views of chicken wire models made to illustrate how lattice discontinuities may be associated with curvature. Elimination of one row of hexagons creates a pentagon and a heptagon with an extra strut, which is also occasionally seen in vivo (cf. Fig. 12, *top*), and creates a slight degree of lattice curvature. Elimination of three rows in a sequential, pie-shaped piece creates one lone pentagon at the apex of a more sharply curved lattice. A pure hexagonal lattice can be rolled into a cylinder, but cannot assume the three-dimensional curves associated with lattice discontinuities.

tightly knit meshwork (Fig. 14*f*). Though this meshwork did not appear as neatly polygonal as it did when viewed from the inside, there was little doubt that it represented an outer view of the coated pits in the plasma membrane. (Indeed, the immunocytochemistry of coated pits with anti-clathrin has been performed on fibroblasts fixed with aldehydes and extracted with Triton X-100 in just this way [4]).

Freeze-Fracturing Coated Pits

Oblique fractures through coated pits were also found. Representative examples are shown in Fig. 16 that illustrate the overall thickness of the coat,

FIGURE 14 Views of the outside of coated pits in the upper plasma membrane of freeze-dried fibroblasts, which display spherical 25-nm droplets thought to be LDL molecules, among other smaller and more irregular surface protrusions. Micrographs *a–c* display the probable sequence of clustering and indentation of LDL-rich patches of membrane, until at *d* the invagination is so deep that the molecules have mostly disappeared. In *e* is shown the etched surface of a quick-frozen fibroblast that was not fixed and freeze-dried from distilled water as were those in *a–d*. LDL molecules are still visible, but are more difficult to see amid the debris that dries onto the membrane surface. In *f* the plasma membrane of a fixed cell was dissolved away with Triton X-100 to expose an external view of the basketworks that underlie the LDL-rich indentations. Bar, 0.1 μm. × 180,000.

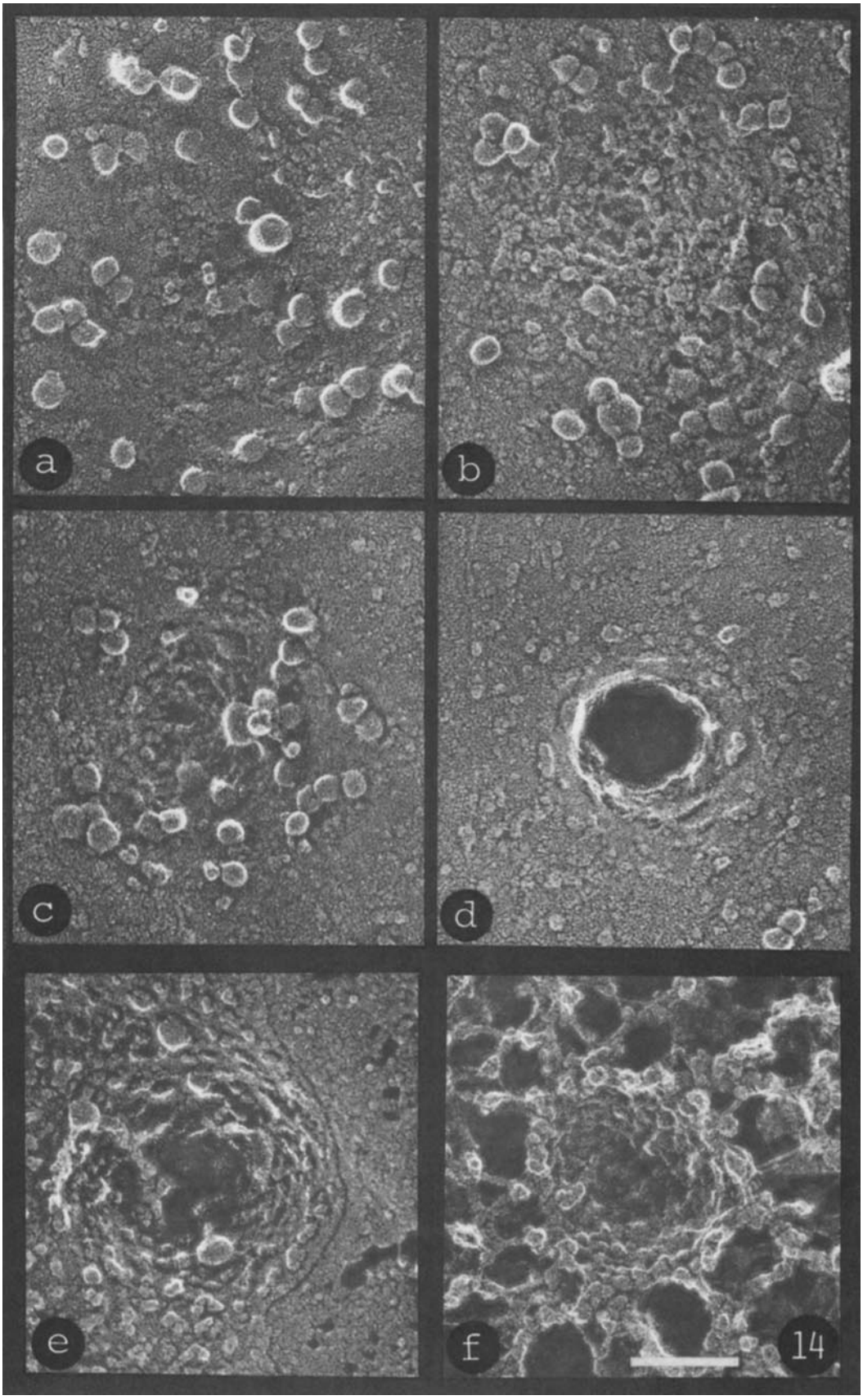
a
b
c
d
e
f
14

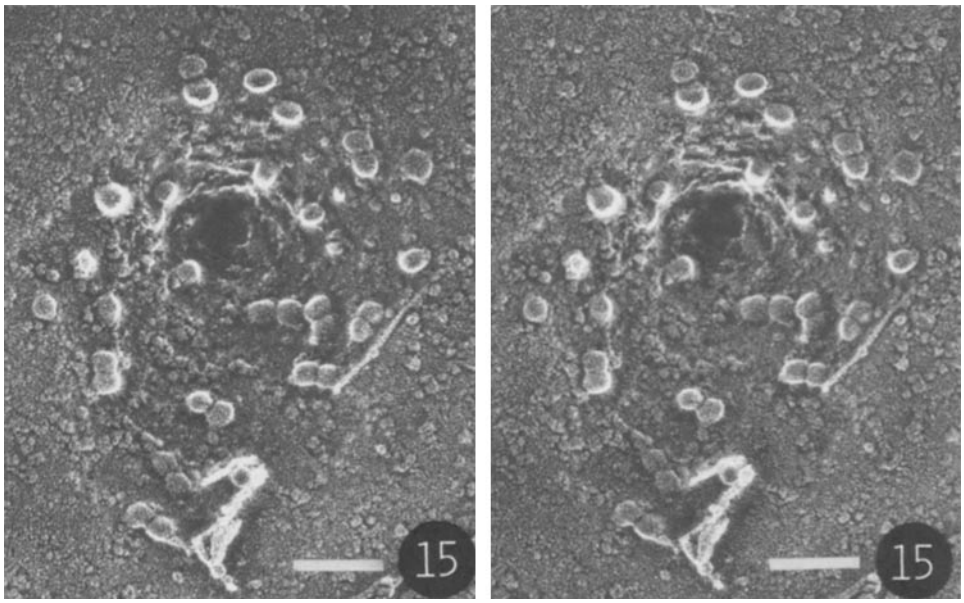

FIGURE 15 Stereo view of one of the droplet-laden indentations that are common on freeze-dried fibroblasts, to show more graphically what are thought to be external views of LDL molecules in coated pits. Bars, 0.1 μm. × 110,000.

or, actually, the separation of the basketwork from the plasma membrane interior exposed during freeze-fracture. Coat thickness measured 190 Å. Coat thickness has been more easily assessed by cutting thin sections through the center of coated pits and measuring the distance from the cytoplasmic interface of the coat to the cytoplasmic dense line of the plasma membrane's "unit" appearance; but, as a result of image superimposition, little has been learned from thin sections about attachments of the coat to the plasma membrane. Unfortunately, the edge views of deep-etched coated pits such as those in Fig. 16 did not reveal much detail either. There was no distinct separation between the inner surface of the plasma membrane and the basketwork itself. It is here that one would expect the plasma membrane receptors for the coat to be found.

Deep-etching of fractured pits such as those in Fig. 16 might also have been expected to have exposed the interfaces of the baskets with the rest of the cytoplasm. Unfortunately, the fibroblasts' cytoplasm proved to be so loaded with unetchable material (cf. reference 40) that very little meaningful detail could actually be seen. The coats seemed to fade off into the surrounding material. This was true also of the isolated baskets seen *in situ* (Fig. 9, *bottom*). In a later paper, we shall show that cells had to be swollen in distilled water or fixed with aldehydes to clear away this unetchable material. Unfortunately, neither of these procedures could be used without damage to the cell. Swelling severely disrupted the normal geometry of the cell and depolymerized the microtubules and some actin filaments. Thus, the absence of discrete attachments to the coated pits (cf. Fig. 1) had to be interpreted with caution. Aldehyde fixation made the unetchable material stick indiscriminately to the formed elements of the cytoplasm and, thus, tended to obscure everything but the coated pits,

FIGURE 16 Edge views of freeze-etched coated pits from unfixed cells, which display the interface between coat and membrane (bracketed in the uppermost micrograph only) and the interface between coat and cytoplasm at the various stages of coated vesicle abscission. Unfortunately, the membranes of these pits have been fractured, so true internal membrane receptors for the coats cannot be seen. It is also unfortunate that the interior of deep-etched cells is so loaded with granular material that apparent attachments to the coat (at arrows) are of dubious significance. Bar, 0.1 μm. × 230,000.

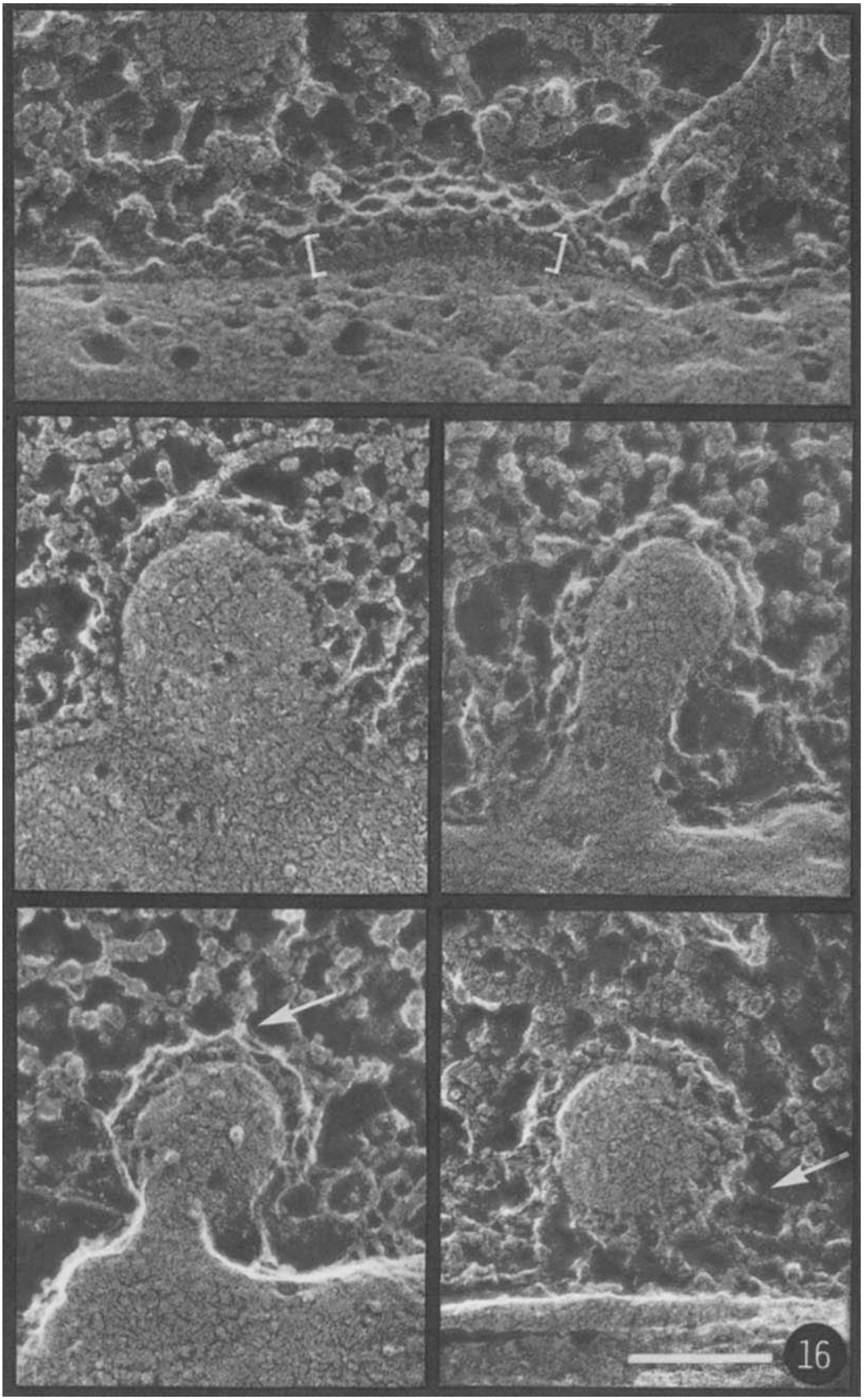
16

which were somehow spared from contamination so that all the images seen in Figs. 2–12 could be obtained. Nevertheless, no particular attachments of cytoplasmic filaments to the basketworks could be found in aldehyde-fixed cells either.

Light microscope immunocytochemistry has shown that coated pits tend to be aligned in rows on the surface of fully spread fibroblasts (4), which raises the possibility that coated vesicle formation is associated with the actin-rich stress fibers that typify these cells. This did not appear to be the case in the fibroblasts studied here. Coated pits seemed to be just as common between the stress fibers as in their immediate vicinity. Fig. 17 shows the only three instances we could find in which coated pits occurred near a submembranous bundle of filaments. This figure also serves as a summary of the various ways of viewing coated pits introduced in this report.

Fig. 17 (*top*) is a view of a fixed cell surface, with the membrane intact and the LDL particles clearly visible in a cuplike depression. Embossed on the plasma membrane of the top of this figure is a granular horizontal band that proved to be a characteristic reflection of an underlying filament bundle. Fig. 17 (*center*) is a view of a fixed cell surface after Triton X-100 extraction in which the plasma membrane and the LDL particles were removed, but the dense meshwork underlying the cuplike depression was retained. Also exposed was a horizontal bundle of cortical microfilaments, seen in the upper portion of the figure. There was no obvious attachment of these submembranous filaments to the adjacent cuplike depression, but something must have held it in place when the membrane was removed. In Fig. 17 (*bottom*), the characteristic inside view of the basketwork from a fixed, fractured, deep-etched cell is shown. Again, a filament bundle was included in the upper portion of this figure to illustrate the only example we could find in which "wisps" appeared to link the basketwork with the submembranous filaments. However, because this cell had been fixed in glutaraldehyde, nothing specific can be said concerning these wisps.

DISCUSSION

Our interest in coated vesicles grew out of observations of membrane recycling at the neuromuscular junction by horseradish peroxidase tracer techniques, which provided evidence that coated vesicles retrieve synaptic vesicle membrane from the plasmalemma after this membrane is added by exocytosis (21). The role of coated vesicles in various sorts of synapses has long been recognized (5, 6, 8, 18–21, 23, 36, 43, 53). Our more recent quick-freezing and freeze-fracture studies have substantiated the idea that coated vesicles are involved in membrane retrieval, and have further indicated that this retrieval is selective by revealing that intramembrane particles that originate in synaptic vesicles and move to the plasma membrane during exocytosis are collected into coated pits before they bud off from the plasma membrane (25, 26). Thus, the formation of coated vesicles at the synapse would appear to be another instance of selective endocytosis, analogous to the process in other cells, where coated vesicles selectively internalize membrane-bound receptors for proteins or hormones as they bud off from the plasma membrane (16).

Furthermore, coated vesicles seem to be involved in a variety of other membrane shuttling pathways inside the cell, all of which involve selection of a particular bit of membrane and transfer to another membrane compartment (13, 42). The coat itself is apparently a ubiquitous apparatus, but what it selects and where it takes the selected membrane inside the cell is highly variable. What is common in every instance is that the coat forms around a specific part of the membrane that is to be budded off. Thus, a role for the coat in budding has been presumed.

Mechanism of Coated Vesicle Formation

The most compelling model showing how this might occur has been provided by Kanaseki and Kadota (29) and is based on their discovery that the coat is a basket of rods or septa linked into hexagons and pentagons. They proposed that this

FIGURE 17 Summary of the three ways of viewing coated pits introduced in this report: (*top*) surface views of freeze-dried whole cells; (*center*) outside views of Triton X-100-extracted cells, and (*bottom*) inside views of freeze-fractured and deep-etched cells. These examples were chosen to illustrate the close association between coated pits and submembranous stress fibers (*SF*) which is occasionally seen (arrow, *bottom*). Bar, 0.1 μm. × 185,000.

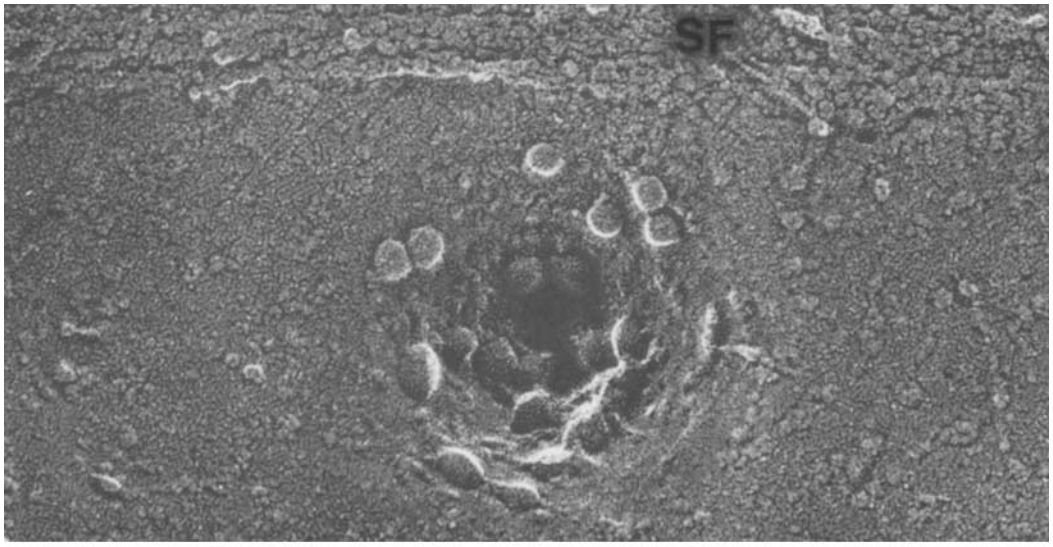
SF

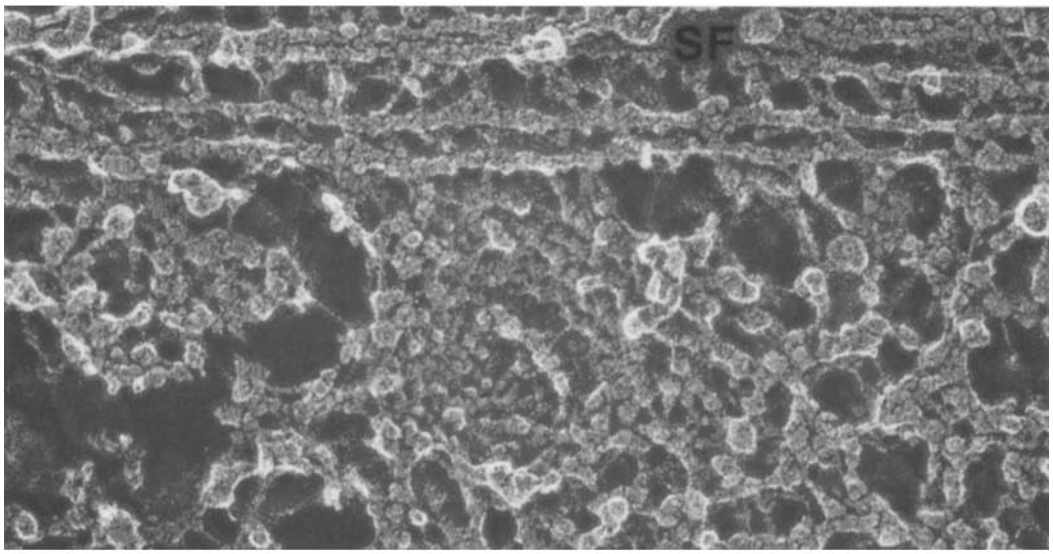
SF

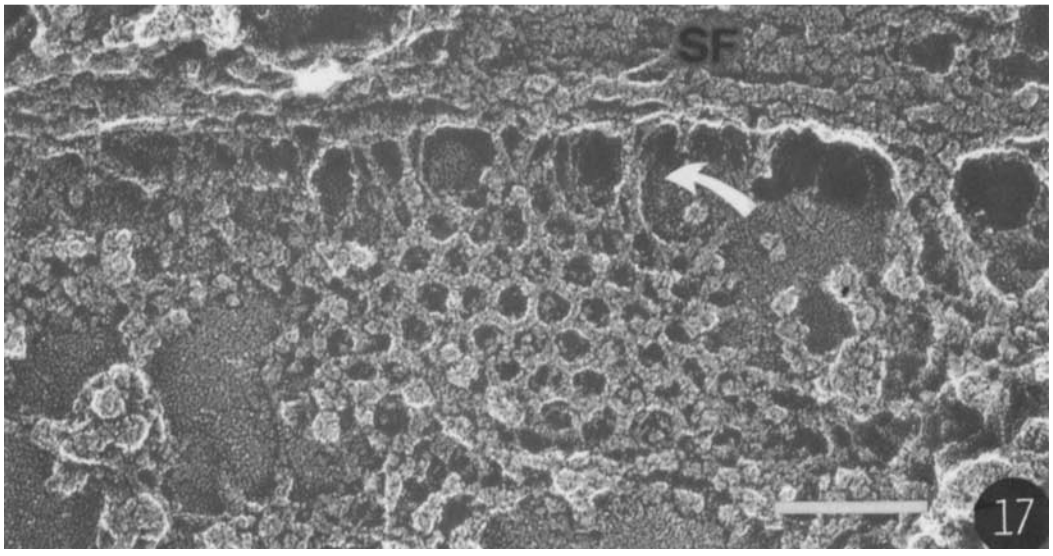
SF
17

basket undergoes internal rearrangements beneath coated pits, that is, transformations of hexagons into pentagons that force the basket and the membrane to curve into a closed vesicle. Indeed, images presented in our report do show a greater proportion of pentagons around closed vesicles than under flat coated pits. Thus, they support Kanaseki and Kadota's idea, but how the transformation occurs is still unknown. They were not necessarily correct in assuming that such a transformation would "power" the vesicle formation; it may be driven by unknown intramembrane forces, and the coat may simply passively comply as the membrane curves.

The images presented here also illustrate that coated pits display a number of five-seven dislocations at contractions and curvatures in the basketwork; these were seen slightly less often in more sharply curved pits and rarely in isolated coated vesicles. Thus, they may be intermediates in the process of coat curvature. Chicken wire models of lattice discontinuities showed considerable strain in the five- and seven-member rings and in the adjacent hexagons. Basketworks with such five-seven pairs may thus tend to rearrange into pure pentagons totally surrounded by hexagons, which, as chicken wire models illustrated, would be less strained internally but much more curved. Crystallography dictates that at least 12 such pentagonal facets must be present in an otherwise hexagonal basketwork for it to curve into a closed sphere.

Mechanism of Coated Vesicle Selectivity

Though it is relatively easy to see how such a structural transformation could be common to a variety of coated vesicle formation, it is more difficult to imagine how this common process achieves the high degree of selectivity that is seen in various situations. Depending on the cell type and the membrane pathways involved, coated vesicles sequester and transport widely differing membrane molecules (see references 2, 11, 12, 17, 26, 52, 54, and 56 for details of various pathways in which coated vesicles are known to be involved). Presumably, these membrane molecules are selected for inclusion in the coated vesicle because they bind directly or indirectly to the coat itself. Indeed, evidence is accumulating that the cell surface receptors that are included by coated vesicles extend through the plasmalemma and possess internal coat-binding sites (1, 3, 4, 16, 34, 35, 51, 52, 54). We are now engaged in an effort to visualize these internal binding sites with the new technique described here by experimentally disassembling the basketworks just before quick freezing.

Recycling and Reassembly of the Coats

There is a little doubt that the basketworks described here can mediate several rounds of coated vesicle formation without new protein synthesis (16), but how they do this is not clear. The simplest possibility would be that they remain permanently associated with a patch of receptor-rich membrane and simply shuttle back and forth between the cell surface and internal compartments. This clearly is not the case in synapses, where very few coated pits and coated vesicles are visible until vesicle membrane is added to the cell surface, after which they appear within seconds (24, 26); nor does it seem to be the case in fibroblasts. Even though the total number of coated pits and coated vesicles does not seem to vary in these cells, receptors can be free from these structures for a significant part of their total lifetime (1, 2, 16). Furthermore, thin sections seem to indicate that, instead of shuttling back and forth intact, the coats fall from the vesicles soon after they have separated from the plasma membrane (2). Also, the method of viewing used in our report illustrates that coats are formed beneath the plasma membrane by progressive expansion by what appears to be piecemeal growth from foci that are initially very small. Thus, recycling of the coats seems to take place by repeated disassembly and reassembly accompanied by a reversible association with the membranes involved, rather than by a permanent shuttling of intact vesicles. This would agree with biochemical findings that isolated coats are held together by noncovalent bonds and can be made to assemble and disassemble by varying their ionic environment (30, 44–46, 50, 55).

It is not known what controls the assembly of coats against certain membranes in vivo, but an interesting lead has been provided by Palade and Fletcher's (42) demonstration that anoxia interrupts coated vesicle formation and makes coat material aggregate into small, empty baskets in pancreatic acinar cells. (After learning of this, we observed that applying metabolic inhibitors to frog nerves produces the same plethora of empty baskets that these authors observed.)

In healthy, quick-frozen cells, these empty baskets are rarely observed but they can quite often be seen in chemically fixed tissues (19, 21) and can be isolated in considerably abundance from homogenized tissues (30, 44–46). Thus, they may be in equilibrium with more soluble coat components in the cytoplasm. If such a soluble pool exists, however, its size remains to be determined. Immunocytochemistry with antibodies against clathrin, the major protein component of the coat, has so far revealed only fully formed coated pits, with very little background staining that might indicate clathrin in the cytoplasm (4). However, the fibroblasts observed so far have been fixed in a manner that may have washed away most of their soluble pool.

The new views on coated pits presented here suggest that a soluble pool of clathrin must exist, and that empty baskets do not contribute directly to the assembly of new coated pits because the coated pit sizes varied (Fig. 4) from just a few facets to hundreds. There was no sign of "quantal jumps" in size, which would be expected if whole baskets were added one at a time, nor was there any sign of empty baskets in the vicinity of newly forming coated pits. Instead, the edges of coated pits were ragged and composed of incomplete polygons, suggesting piecemeal assembly. Thus, the empty basket may be a red herring.

Size vs. Organization of Baskets

In spite of their dubious biological significance, empty baskets have been useful for illustrating how the overall basketwork can be woven of pentagons and hexagons (20) in that empty baskets are just the right size for good negative staining. The only problem has been that such staining invariably reveals both their front and back sides and creates patterns of superimposition that are difficult to interpret (9, 29, 30, 44–46). The surface replication technique used here shows only the front side of the baskets, and, thus, quite simply confirms the structural analyses previously done by laborious comparisons of negatively stained images with computer generated models (9). The smallest empty baskets are about 48 nm in diameter and appear to be composed of 16 facets, 12 pentagons and 4 hexagons in a tetrahedral arrangement. The largest empty baskets are about 55 nm in diameter and appear to be composed of 20 facets, 12 pentagons and 8 hexagons, arranged as barrels and other slightly asymmetric forms. In contrast, the smallest intact coated vesicles are about 75 nm (because the smallest possible membrane vesicle is about 40 nm, and the coat extends from the membrane ~20 nm on all sides.) Such coated vesicles appear to be composed of 32 facets, 12 pentagons and 20 hexagons, arranged in a symmetrical icosahedral pattern. (These were the sort originally recognized in brain homogenates by Kanaseki and Kadota [29]. They can be quite clearly seen in our deep-etched replicas but could not be very clearly seen in previous negative-stain studies [9] because of problems with collapse of the internal vesicle.) The largest coated vesicles, typical of those found in fibroblasts, are greater than 100 nm in diameter and have more than 100 facets, of which only about 10% are pentagons (though the total number of pentagons must presumably still be 12 to form a closed, spherical surface). These are much too large to image by negative staining because they collapse (cf. Fig. 2 in reference 46) but can clearly be seen by the method we used.

Protein Composition of Baskets

Though clathrin is the major component of isolated baskets (44, 45), and though baskets can be formed in vitro from pure clathrin (30), the baskets around coated vesicles in vivo appear to contain at least two other proteins (30, 46, 55). These proteins exert strong influences on the tendency of clathrin to polymerize in vitro. The stoichiometric ratios of these accessory proteins vs. clathrin suggests that they may help to form the vertices of the baskets, where three clathrin molecules presumably come together (30, 46).

Our current efforts are directed toward identifying the location of these accessory proteins by direct visualization of antibodies bound to them. We will show that the new viewing technique used here allows sufficient resolution to visualize IgG molecules directly, without the need for accessory electron-dense tags (J. Heuser and M. W. Kirschner, manuscript submitted). Thus, the technique should be useful for identifying the protein composition of the basketworks it reveals so clearly.

Heartiest thanks to Marc Kirschner and Margaret Lopata, Department of Biochemistry, University of California, San Francisco, for supplying the fibroblasts and to Lou Reichardt and Carol Lopez, Division of Neurobiology, University of California, San Francisco, for

supplying the coated vesicles purified from brain. Thanks also to Richard Anderson and Jim Rothman for helpful discussion. Frank McKeon performed the quantitation and statistics in this study.

This work was supported by grants from the Muscular Dystrophy Association of America and the U. S. Public Health Service (NS-11979).

Received for publication 13 August 1979, and in revised form 7 November 1979.

REFERENCES

1. ANDERSON, R. G. W., J. L. GOLDSTEIN, and M. S. BROWN. 1976. Localization of low density lipoprotein receptors on plasma membrane of normal human fibroblasts and their absence in cells from a familial hypercholesterolemia homozygote. *Proc. Natl. Acad. Sci. U. S. A.* **73:** 2434–2438.
2. ANDERSON, R. G. W., M. S. BROWN, and J. L. GOLDSTEIN. 1977. Role of the coated endocytic vesicle in the uptake of receptor bound low density lipoprotein in human fibroblasts. *Cell.* **10:**351–364.
3. ANDERSON, R. G. W., J. L. GOLDSTEIN, and M. S. BROWN. 1977. A mutation that impairs the ability of lipoprotein receptors to localise in coated pits on the cell surface of human fibroblasts. *Nature (Lond.).* **270:**695–699.
4. ANDERSON, R. G. W., E. VASILE, R. J. MELLO, M. S. BROWN, and J. L. GOLDSTEIN. 1978. Immunocytochemical visualization of coated pits and vesicles in human fibroblasts: relation to low density lipoprotein receptor distribution. *Cell.* **15:**919–933.
5. ANDRES, K. H. 1964. Mikropinozytose im Zentralnervensystem. *Z. Zellforsch. Mikrosk. Anat.* **64:**63–73.
6. BENEDECZKY, I., and A. D. SMITH. 1972. Ultrastructural studies on the adrenal medulla of golden hamster: origin and fate of secretory granules. *Z. Zellforsch. Mikrosk. Anat.* **124:**367–386.
7. BOWERS, B. 1964. Coated vesicles in the pericardial cells of the aphid. *Protoplasma.* **59:**351–367.
8. BUNT, A. H. 1969. Formation of coated and "synaptic" vesicles within neurosecretory axon terminals of the crustacean sinus gland. *J. Ultrastruct. Res.* **28:**411–421.
9. CROWTHER, R. A., J. T. FINCH, AND B. M. F. PEARSE. 1976. On the structure of coated vesicles. *J. Mol. Biol.* **103:**785–798.
10. DROLLER, M. J., and T. F. ROTH. 1966. An electron microscope study of yolk formation during oogenesis in *Clebistes reticulatus* guppyi. *J. Cell Biol.* **28:**209–232.
11. FARQUHAR, M. G. 1978. Recovery of surface membrane in anterior pituitary cells. Variations in traffic detected with anionic and cationic ferritin. *J. Cell Biol.* **77:**R35–R42.
12. FARQUHAR, M. G. 1978. Traffic of products and membranes through the Golgi complex. *In* Transport of Macromolecules in Cellular Systems. S. C. Silverstein, editor. Dahlem Konferenzen, Berlin. 341–362.
13. FRIEND, D. S., and M. G. FARQUHAR. 1967. Functions of coated vesicles during protein absorption in the rat vas deferens. *J. Cell Biol.* **35:**357–376.
14. FAWCETT, D. W. 1964. Local specializations of the plasmalemma in micropinocytosis vesicles of erythroblasts. *Anat. Rec.* **148:**370–389.
15. FAWCETT, D. W. 1964. Surface specialization of absorbing cells. *J. Histochem. Cytochem.* **13:**75–98.
16. GOLDSTEIN, J. L., R. G. W. ANDERSON, and M. S. BROWN. 1979. Coated pits, coated vesicles, and receptor-mediated endocytosis. *Nature (Lond.).* **279:**679–685.
17. GORDEN, P., J.- L. CAPRENTIER, S. COHEN, and L. ORCI. 1978. Epidermal growth factor: morphological demonstration of binding, internalization, and lysosomal association in human fibroblasts. *Proc. Natl. Acad. Sci. U. S. A.* **75:**5025–5029.
18. GRAY, E. G. 1961. The granule cells, mossy synapses and Purkinje spine synapses of the cerebellum: light and electron microscope observations. *J. Anat.* **95:**345–356.
19. GRAY, E. G. 1972. Are the coats of coated vesicles artefacts? J. *Neurocytol.* **1:**363–382.
20. GRAY, E. G., and H. PEASE. 1971. On understanding the organization of the retinal receptor synapses. *Brain Res.* **35:**1–15.
21. GRAY, E. G., and R. A. WILLIS. 1970. On synaptic vesicles, complex vesicles and dense projections. *Brain Res.* **24:**149–168.
22. GULIK-KRZYWICKI, T., M. YATES. and L. AGGERBECK. 1979. The use of freeze-etching electron microscopy to study biological molecules in solution. Application to the study of human serum lipoproteins. *J. Mol. Biol.* In press.
23. HAMA, K., and K. SAITO. 1977. Fine structure of the afferent synapse of the hair cells in the saccular macula of the goldfish, with special reference to anastomosing tubules. *J. Neurocytol.* **6:**361–373.
24. HEUSER, J. E., and T. S. REESE. 1973. Evidence for recycling of synaptic vesicle membrane during transmitter release at the frog neuromuscular junction. *J. Cell Biol.* **57:**315–344.
25. HEUSER, J. E., and T. S. REESE. 1975. Redistribution of intramembranous particles from synaptic vesicles: direct evidence for vesicle recycling. *Anat. Rec.* **181:**374.
26. HEUSER, J. E., and T. S. REESE. 1979. Synaptic vesicle exocytosis captured by quick freezing. *In* The Neurosciences, Fourth Study Program. F. O. Schmitt and F. G. Wordin, editor. MIT Press, Cambridge, Mass. 573–600.
27. HEUSER, J. E., T. S. REESE, M. J. DENNIS, Y. JAN., L. JAN, and L. EVANS. 1979. Synaptic vesicle exocytosis captured by quick freezing and correlated with quantal transmitter release. *J. Cell Biol.* **81:**275–300.
28. HEUSER, J. E., and S. R. SALPETER. 1979. Organization of acetylcholine receptors in quick-frozen, deep-etched, and rotary-replicated "torpedo" postsynaptic membrane. *J. Cell Biol.* **82:**150–173.
29. KANASEKI, T., and K. KADOTA. 1969. The "vesicle in a basket." A morphological study of the coated vesicle isolated from the nerve endings of the guinea pig brain, with special reference to the mechanism of membrane movements. *J. Cell Biol.* **42:**202–220.
30. KEEN, J. H., M. C. WILLINGHAM, and I. H. PASTAN. 1979. Clathrin-coated vesicles: isolation, dissociation and factor-dependent reassociation of clathrin baskets. *Cell.* **16:**303–312.
31. KESSEL, R. G. 1968. An electron microscope study of differentiation and growth in oocytes of *Ophioderma panamensis. J. Ultrastruct. Res.* **22:**63–78.
32. KRAEHENBUHL, J. P., Y. SUARD, and L. KÜHN. 1977. Specific uptake of secretory immunoglobulins by mammary epithelial cells. *J. Cell Biol.* **75**(2, Pt. 2):362*a* (Abstr.).
33. MAUNSBACH, A. B. 1966. Absorption of ferritin by rat kidney proximal tubule cells: electron microscopic observations of the initial uptake phase in cells of microperfused single proximal tubules. *J. Ultrastruct. Res.* **16:**1–37.
34. MAXFIELD, F. R., J. SCHLESSINGER, Y. SHECHTER, I. PASTAN, and M. C. WILLINGHAM. 1978. Collection of insulin, EGF and α_2-macroglobulin in the same patches on the surface of cultured fibroblasts and common internalization. *Cell.* **14:**805–810.
35. MAXFIELD, F. R., M. C. WILLINGHAM, P. J. A. DAVIES, and I. PASTAN. 1979. Amines inhibit the clustering of α_2 macroglobulin and EGF on the fibroblast cell surface. *Nature (Lond.).* **277:**661–662.
36. NAGASAWA, J., W. W. DOUGLAS, and R. A. SCHULTZ. 1971. Micropinocytotic origin of coated and smooth microvesicles ("synaptic vesicles") in neurosecretory terminals of posterior pituitary glands demonstrated by incorporation of horseradish peroxidase. *Nature (Lond.).* **232:**341–343.
37. OCKLEFORD, C. D. 1976. A three-dimensional reconstruction of the polygonal pattern on placental coated-vesicle membranes. *J. Cell Sci.* **21:**83–91.
38. OCKLEFORD, C. D., and G. MENON. 1977. Differentiated regions of human placental cell surface associated with exchange of materials between maternal and foetal blood: a new organelle and the binding of iron. *J. Cell Sci.* **25:**279–291.
39. OCKLEFORD, C. D., and A. WHYTE. 1977. Differentiated regions of human placental cell surface associated with exchange of materials between maternal and foetal blood: coated vesicles. *J. Cell Sci.* **25:**293–312.
40. OHTSUKI, I., R. M. MANZI, G. E. PALADE, and J. D. JAMIESON. 1978. Entry of macromolecular tracers into cells fixed with low concentrations of aldehydes. *Biol. Cell.* **31:**119–126.
41. ORCI, L., J. L. CARPENTER, A. PERRELET, R. G. W. ANDERSON, J. L. GOLDSTEIN, and M. S. BROWN. 1978. Occurrence of low density lipoprotein receptors within large pits on the surface of human fibroblasts as demonstrated by freeze-etching. *Exp. Cell Res.* **113:**1–13.
42. PALADE, G. E., and M. FLETCHER. 1977. Reversible alterations in the morphology of the Golgi complex induced by the arrest of secretory transport. *J. Cell Biol.* **75**(2, Pt. 2):371*a* (Abstr.).
43. PALAY, S. L. 1963. Alevolate vesicles in Purkinje cells of the rat's cerebellum. *J. Cell Biol.* **19:**89A (Abstr.).
44. PEARSE, B. M. F. 1975. Coated vesicles from pig brain: purification and biochemical characterization. *J. Mol. Biol.* **97:**93–98.
45. PEARSE, B. M. F. 1976. Clathrin: a unique protein associated with intracellular transfer of membrane by coated vesicles. *Proc. Natl. Acad. Sci. U. S. A.* **73:**1255–1259.
46. PEARSE, B. M. F. 1978. On the structural and functional components of coated vesicles. *J. Mol. Biol.* **126:**803–812.
47. RODEWALD, R. B. 1973. Intestinal transport of antibodies in the newborn rat. *J. Cell Biol.* **58:**189–211.
48. ROSENBLUTH, J., AND S. L. WISSIG. 1964. The uptake of ferritin by toad

spinal ganglion cells. *J. Cell Biol.* **23**:307–325.
49. ROTH, T. F., and K. R. PORTER. 1964. Yolk protein uptake in the oocyte of the mosquito *Aedes aegypti* L. *J. Cell Biol.* **20**:313–332.
50. ROTH, T. F., J. A. CUTTING, and S. B. ATLAS. 1976. Protein transport: a selective membrane mechanism. *J. Supramol. Struct.* **4**:527(487)-548(508).
51. SCHECHTER, Y., L. HERNAEZ, J. SCHLESSINGER, and P. CUATRECASAS. 1979. Local aggregation of hormone-receptor complexes is required for activation by epidermal growth factor. *Nature (Lond.)*. **278**:835–838.
52. SCHLESSINGER, J., Y. SCHECHTER, M. C. WILLINGHAM, and I. PASTAN. 1978. Direct visualization of the binding, aggregation, and internalization of insulin and epidermal growth factor on fibroblastic cells. *Proc. Natl. Acad. Sci. U. S. A.* **75**:2659–2663.
53. WESTRUM, L. E. 1965. On the origin of synaptic vesicles in the cerebral cortex. *J. Physiol. (Lond.)*. **179**:4P–6P.
54. WILLINGHAM, M. C., F. R. MAXFIELD, and I. H. PASTAN. 1979. α_2Macroglobulin binding to the plasma membrane of cultured fibroblasts. *J. Cell Biol.* **82**:614–625.
55. WOODS, J. W., M. P. WOODWARD, and T. F. ROTH. 1978. Common features of coated vesicles from dissimilar tissues: composition and structure. *J. Cell Sci.* **30**:87–97.
56. YOUNGDAHL-Turner, P., L. E. Rosenberg, and R. H. ALLEN. 1978. Binding and uptake of transcobalamin II by human fibroblasts. *J. Clin. Invest.* **61**:133–141.